ELSEVIER

Journal of Power Sources 92 (2001) 244–249

JOURNAL OF POWER SOURCES

www.elsevier.com/locate/jpowsour

Synthesis and electrochemical characterization of $Li_{1.02}Mg_{0.1}Mn_{1.9}O_{3.99}S_{0.01}$ using sol–gel method

Sang Ho Park[a], Ki Soo Park[a], Sung Sik Moon[a], Yang Kook Sun[b], Kee Suk Nahm[a,*]

[a]*School of Chemical Engineering and Technology, College of Engineering, Chonbuk National University, Chonju 561-756, South Korea*
[b]*Department of Industrial Chemistry, College of Engineering, Hanyang University, Seoul 133-791, South Korea*

Received 12 May 2000; accepted 3 July 2000

Abstract

To improve the cycle performance of spinel $LiMn_2O_4$ as the positive electrode of 4 V lithium secondary batteries, the spinel oxysulfide $Li_{1.02}Mg_{0.1}Mn_{1.9}O_{3.99}S_{0.01}$ is synthesized by a sol–gel method using adipic acid as a chelating agent. The structural and electrochemical properties of the synthesized material are examined. Highly crystallized $Li_{1.02}Mg_{0.1}Mn_{1.9}O_{3.99}S_{0.01}$ is synthesized at 750°C in an oxygen atmosphere. Both cation and anion doping of spinel lithium manganese oxides are very effective for improving the cycle performance of lithium batteries.

Keywords: Spinel oxysulfide; Sol–gel method; Manganese oxide; Lithium-ion battery; Magnesium and sulfur doping

1. Introduction

An enormous growth in portable electronic devices, such as cellular phones and laptop computers has led to an increasing demand for compact lightweight batteries with high energy and power capability [1,2]. Lithium secondary batteries have satisfied this demand to a greater degree than other rechargeable battery systems [3,4].

Recently, the spinel $LiMn_2O_4$ and its derivatives have been studied as 4 V positive-electrode materials for lithium secondary batteries because of their low cost, abundance, and non-toxicity [4,5]. The wider use of these materials has been limited, however, because of their poor cycling performance. In the charge and discharge processes, lithium ions are reversibly inserted into and extracted out of the $Li_xMn_2O_4$ spinel phase in two composition ranges, viz. $0 \leq X \leq 1$ and $1 \leq X \leq 2$ which induce two voltage plateaux at 4 and 3 V, respectively [6,7]. It has been proposed that the reasons for the capacity fading are instability of the organic-based electrolyte and dissolution of the electrode surface in electrolyte at 4 V [6–10], and severe crystallographic Jahn-Teller distortions at 3 V [11].

Several research groups have attempted to stabilize the structure of $LiMn_2O_4$ powders during cycling at 4 V by substituting a small fraction of the manganese ions with other metal cations, such as Al, Ni, Cr, and Co [12–15]. They have consistently achieved substantial reduction in capacity fade. It has been reported that these admetals replace Mn^{3+} at 16d octahedral sites to enhance lattice disorder by preferring tetrahedral coordination. In other work, a few researchers have shown that the capacity loss of $LiMn_2O_4$ electrode is minimized by replacing a small amount of the oxygen ions with other anions [16,17].

In this study, we have synthesized spinel oxysulfide $Li_{1.02}Mg_{0.1}Mn_{1.9}O_{3.99}S_{0.01}$ powders using a sol–gel method and have evaluated the electrochemical performance. The structural and electrochemical properties of the synthesized powders are measured and correlated to explain the electrochemical activity of the materials. The effect of Mg and S doping in $LiMn_2O_4$ is examined as function of the amounts of Mg and S dopant.

2. Experimental

$Li_{1.02}Mg_xMn_{2-x}O_{4-y}S_y$ powders were synthesized as a function of the doped amount of Mg and S using a sol–gel method. The detailed synthetic procedure has been reported in our previous work [18]. For example, $Li_{1.05}Mg_{0.1}Mn_{1.9}O3.9S_{0.1}$ powder, which is a composition for calculating the ratio of starting materials, was prepared as follows. A stoichiometric amount of lithium acetate

* Corresponding author. Tel.: +82-652-270-2311; fax: +82-652-270-2306.
E-mail address: nahmks@moak.chonbuk.ac.kr (K.S. Nahm).

0378-7753/01/$ – see front matter
PII: S0378-7753(00)00545-0

($Li(CH_3COO)\cdot 2H_2O$), magnesium acetate ($Mg(CH_3COO)_2\cdot 4H_2O$), manganese acetate ($Mn(CH_3COO)_2\cdot 4H_2O$) and lithium sulfide (Li_2S) (Li:Mg:Mn:Li = 0.75:0.1:1.9:0.3) was dissolved in distilled water. The dissolved solution was slowly introduced into a continuously agitated aqueous solution of adipic acid. Adipic acid was used as a chelating agent for the synthetic reaction. The molar ratio of adipic acid to total metal ions was fixed at unity. The pH of the mixed solution was adjusted to be in the range 4.5–3.0 by adding acetic acid. The prepared solution was evaporated in the temperature range 90–100°C for 8 h to produce a transparent sol. As water evaporated further, the sol was transformed into a viscous transparent gel. The resulting gel precursors were heated at a temperature ramping rate of 1°C/min and decomposed at 450°C for 10 h in air to eliminate organic components. The decomposed powders were moved into a tubular electrical furnace and calcined at 750°C under a flow of oxygen (2500 sccm) for 14 h. Both heating and cooling rates were 1°C/min to prevent cation mixing in $Li_{1.05}Mg_{0.1}Mn_{1.9}O_{3.9}S_{0.1}$. The real composition of the synthesized material was determined as $Li_{1.02}Mg_{0.1}Mn_{1.9}O_{3.99}S_{0.01}$ by chemical analysis. Other doped manganese oxides were synthesized via the same process by manipulating the stoichiometric composition of the corresponding starting materials.

X-ray diffraction (XRD, D/Max-3A, Rigaku) measurements using Cu Kα radiation was used to investigate the structural properties of the synthesized powders. The particle morphology of the powders was observed with a scanning electron microscope (SEM, GEOL, JSM 6400). Rietveld refinement of the XRD data was performed to measure the lattice constant *a* of the synthesized powders.

The electrochemical properties of $Li_{1.02}Mg_xMn_{2-x}O_{4-y}S_y$ powders were measured in a three-electrode cell. An excess amount of lithium foil was used as the negative electrode. The electrolyte was a 1:1 mixture of ethylene carbonate (EC) and diethyl carbonate (DEC) that contained 1 M $LIBF_4$ (Mitsubishi Co.). The positive electrode was a mixture of 72 wt.% active material, 20 wt.% ketjenblack EC, and 8 wt.% Teflon binder. The mixture was dispersed in isopropyl alcohol and spread on Exmet, followed by pressing and drying at 120°C for 5 h in an vacuum oven. After the cells were assembled in a argon-filled dry box, charge-discharge cycling was galvanostatically performed at a current density of 1 mA cm^{-2} (a rate of 0.5 C) with a cut-off voltage of 3.0–4.4 V (versus Li/Li^+).

3. Results and discussion

3.1. Structural characterization of $Li_{1.02}Mg_xMn_{2-x}O_{4-y}S_y$

Data from chemical analysis indicated that the real composition of the synthesized powders was $Li_{1.02}Mg_{0.1}Mn_{1.9}O_{3.99}S_{0.01}$. The average oxidation state of manganese in the sample was 3.57. This was measured by a potentiometric titration method given in the literature [19].

In order to determine the doping effect of cations (Mn) and anions (O) on the structural and electrochemical properties of spinel $LiMn_2O_4$, cations and anions were partially substituted with Mg and S, respectively. The XRD patterns for $Li_{1.02}Mn_2O_4$, $Li_{1.02}Mg_{0.1}Mn_{1.9}O_4$, $Li_{1.02}Mn_2O_{3.99}S_{0.01}$ and $Li_{1.02}Mg_{0.1}Mn_{1.9}O_{3.99}S_{0.01}$ powders are shown in Fig. 1. The XRD analysis indicates that all samples are identified as a single-phase spinel with a space group *Fd3m* in which the lithium ions occupy the tetrahedral (8a) sites and the transition metal ions reside at the octahedral (16d) sites [20]. The sharp (4 0 0) peak of all the samples reveals that highly crystallized manganese oxides had been synthesized [21].

The morphology of the synthesized powders was observed by means of scanning electron microscopy (SEM). Electron micrographs of the powders prepared under the same conditions of Fig. 1 are shown in Fig. 2. For $Li_{1.02}Mn_2O_4$ powders (Fig. 2(a)), the shape is polygonal as seen for the solid-state reaction method [21] and the average particle size is about 0.5 μm with a fairly narrow size-distribution. The shape of the doped powders is quite different from that of $Li_{1.02}Mn_2O_4$. $Li_{1.02}Mg_{0.1}Mn_{1.9}O_4$ particles have a rectangular structure with an average particle size of 0.5 μm, as shown in Fig. 2(b). By contrast, the morphology of sulfur-doped powders (Fig. 2(c) and (d)) is analogous to that of single-crystal gold with a cubic struc-

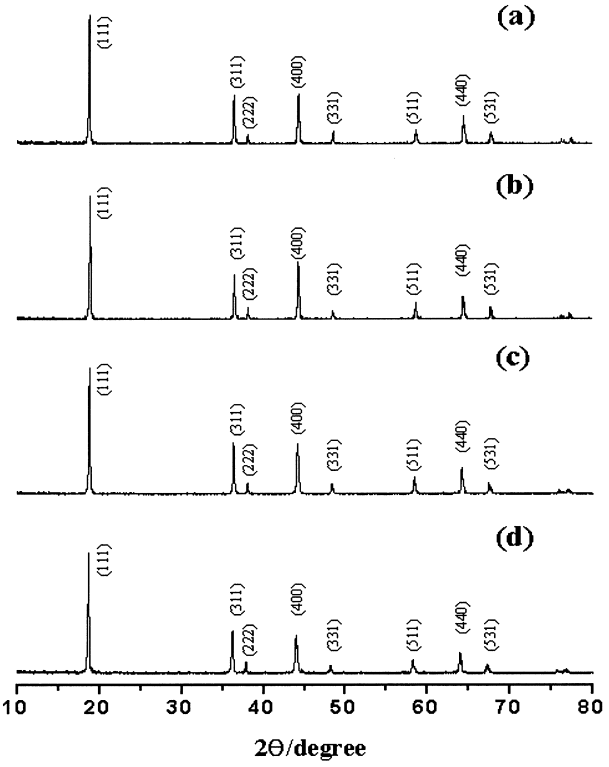

Fig. 1. X-ray diffraction patterns of $Li_{1.02}Mg_xMn_{2-x}O_{4-y}S_y$ powders prepared as function of *x* and *y* contents. The gel precursors were calcined at 750°C in O_2: (a) $Li_{1.02}Mn_2O_4$; (b) $Li_{1.02}Mg_{0.1}Mn_{1.9}O_4$; (c) $Li_{1.02}Mn_2O_{3.99}S_{0.01}$; (d) $Li_{1.02}Mg_{0.1}Mn_{1.9}O_{3.99}S_{0.01}$ powders.

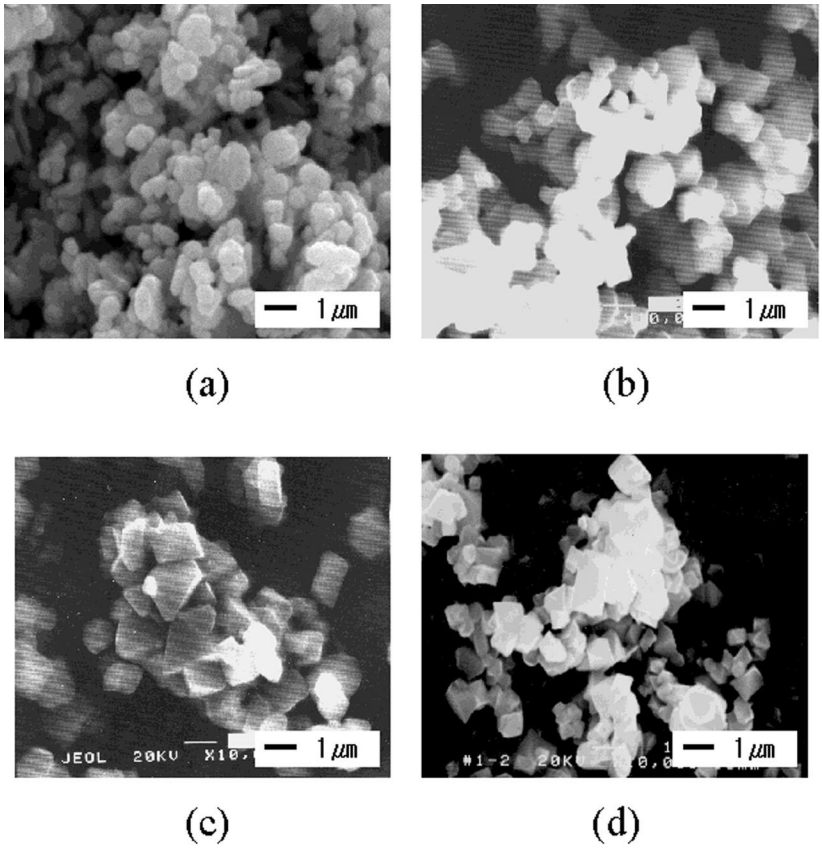

Fig. 2. Scanning electron micrographs for (a) $Li_{1.02}Mn_2O_4$; (b) $Li_{1.02}Mg_{0.1}Mn_{1.9}O_4$; (c) $Li_{1.02}Mn_2O_{3.99}S_{0.01}$; (d) $Li_{1.02}Mg_{0.1}Mn_{1.9}O_{3.99}S_{0.01}$ powders.

ture. The particles have a well-developed octahedral structure which is bounded by eight (1 1 1) planes. The size distribution ranges from 0.5 to 1.5 μm. In addition, the particle size of $Li_{1.02}Mn_2O_{3.99}S_{0.01}$ powders is larger than that of $Li_{1.02}Mn_2O_4$. At present, it is not clear how the size and morphology of the particles influence the capacity of the electrode, but it is speculated that the sulfur acts as a catalyst in the synthetic process of S-doped Mn phase to increase the particle size and enhance the stability of the structure. The catalytic activity of sulfur in the oxidation process of metals has been reported by others [22].

The lattice constant *a* of the cubic unit cell for the materials prepared under the synthetic conditions of Fig. 1 was calculated by Rietveld refinement using measured XRD data. The results for each sample are given in Fig. 3. The lattice constant *a* of typical $LiMn_2O_4$ powders has been reported as 8.2342 Å, which is nearly equal to that of the samples in this study. The lattice parameter *a* decreases slightly from 8.23 to 8.18 Å for powders in the order: $Li_{1.02}Mn_2O_4$, $Li_{1.02}Mg_{0.1}Mn_{1.9}O_4$, $Li_{1.02}Mn_2O_{3.99}S_{0.01}$, and $Li_{1.02}Mg_{0.1}Mn_{1.9}O_{3.99}S_{0.01}$. This progressive decrease in the unit-cell dimension of the Mg-doped materials may be due to an increase in the percentage of smaller Mn^{4+} ions in the structure as the amount of doped divalent Mg increases. The average oxidation state of $Li_{1.02}Mg_{0.1}Mn_{1.9}O_4$ measured by a potentiometric titration method is 3.57, which indicates the increase of Mn^{4+} ions in the prepared samples. For S-doped manganese oxides, on the other hand, it is considered that the sulfur might enhance the Mn–O bonding strength due to the catalytic activity of sulfurs for the formation of metal oxides, which results in the reduction of the lattice constant [22].

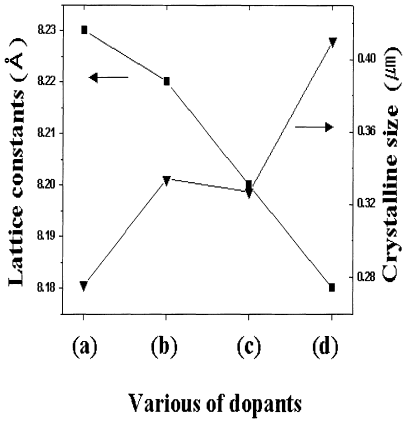

Fig. 3. Lattice constant *a* and crystalline size as a function of various dopants: (a) $Li_{1.02}Mn_2O_4$; (b) $Li_{1.02}Mg_{0.1}Mn_{1.9}O_4$; (c) $Li_{1.02}Mn_2O_{3.99}S_{0.01}$; (d) $Li_{1.02}Mg_{0.1}Mn_{1.9}O_{3.99}S_{0.01}$ powders.

Many researchers have reported that the cubic lattice parameter and unit cell volume of spinel lithium manganese oxides changes when Mn is partially substituted with some transition metal dopants. Moreover, the magnitude of the change is mainly dependent on the atomic properties of the dopants. Tarascon et al. [23] reported that the lattice constant a of doped $LiMn_2O_4$ increases in the order: titanium, germanium, nickel, zinc, and iron. It was also revealed [23,24] that an additional change in the lattice parameter occurs as the amount of dopant increases. For magnesium dopant, it was observed that the lattice parameter decreases because of a contraction of the spinel crystal structure. Tarascon et al. [23] discussed that the $Li_xMn_2O_4$ powders display excellent electrochemical properties when the lattice parameter is less than about 8.23 Å and the powders have nominal formulations with x greater than about 1.0 in $Li_xMn_2O_4$.

The crystalline size of the materials prepared under the conditions of Fig. 1 was calculated by applying the Scherrer equation to the full-width half-maximum (FWHM) values of the (4 0 0) peaks in Fig. 1. The results are presented in Fig. 3 for each material [25]. The crystalline size of the materials varies in the reverse manner as the lattice constant shown in Fig. 3. The crystalline size for the particles varies from 0.276 to 0.41 μm. It is well known that the crystalline size or the width of the Bragg peaks for a given material relates to the presence of residual strain, and is inversely proportional to this strain. A lower crystalline size may result from defects, such as composition inhomogeneities, cationic mixing, grain boundaries, or polymorphism [26,27].

To investigate the effect of the amount of doped Mg on the structure of $LiMn_2O_4$, $Li_{1.02}Mg_xMn_{2-x}O_{3.99}S_{0.01}$ powders were synthesized as a function of this amount and the structure of each powder was characterized by means of X-ray diffraction. The XRD patterns for the synthesized $Li_{1.02}Mg_xMn_{2-x}O_{3.99}S_{0.01}$ ($x = 0.1-0.3$) powders are given in Fig. 4. For $x = 0.1$ (Fig. 4(a)), the powders have a typical spinel $LiMn_2O_4$ structure, which indexes to a cubic unit cell with a space group $Fd3m$. As the doped amount of Mg is increased further, however, the splitting of (3 1 1) and (4 0 0) peaks begins to occur and peaks related to impurities appear in the 2Θ range of 10–40°. This indicates that the crystallinity of $LiMn_2O_4$ deteriorates with increase in the amount of Mg dopant.

$Li_{1.02}Mg_{0.1}Mn_{1.9}O_{4-y}S_y$ powders were also synthesized as a function of the doped amount of S to study the effect on the structure of $LiMn_2O_4$. The XRD patterns for $Li_{1.02}Mg_{0.1}Mn_{1.9}O_{4-y}S_y$ powders prepared as a function of the doped amount of S ($y = 0.01-0.03$) are presented in Fig. 5. An increase in the amount of S causes the splitting of (3 1 1) and (4 0 0) peaks, as observed in Fig. 4, while the formation of impurities is suppressed. This indicates he existence of two phases in the synthesized $LiMn_2O_4$ powders, which results in a deterioration of the electrochemical properties of the materials. In addition, it is likely that the amount of doped Mg has a severe impact on the

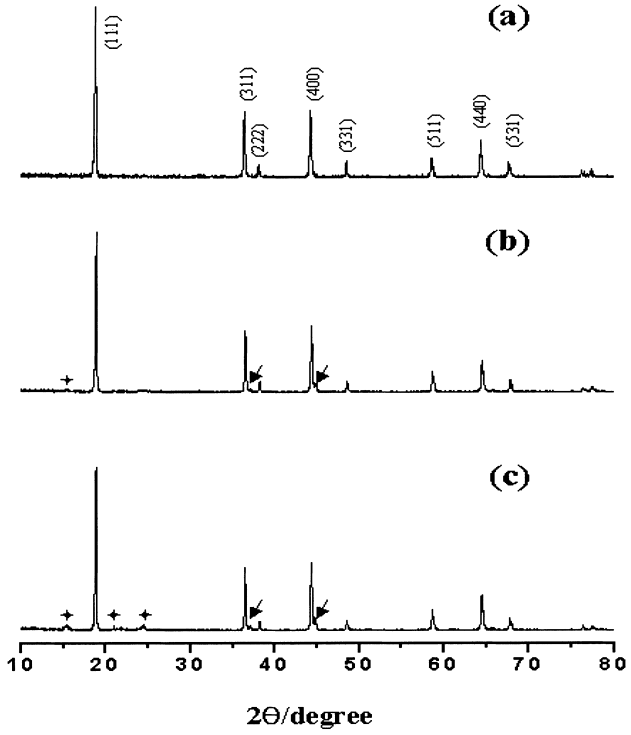

Fig. 4. X-ray diffraction patterns of $Li_{1.02}Mg_xMn_{2-x}O_{3.99}S_{0.01}$ powders prepared at various magnesium contents. Gel precursors were calcined at 750°C in O_2: (a) $Li_{1.02}Mg_{0.1}Mn_{1.9}O_{3.99}S_{0.01}$; (b) $Li_{1.02}Mg_{0.2}Mn_{1.8}O_{3.99}S_{0.01}$; (c) $Li_{1.02}Mg_{0.3}Mn_{1.7}O_{3.99}S_{0.01}$ + unknown peaks.

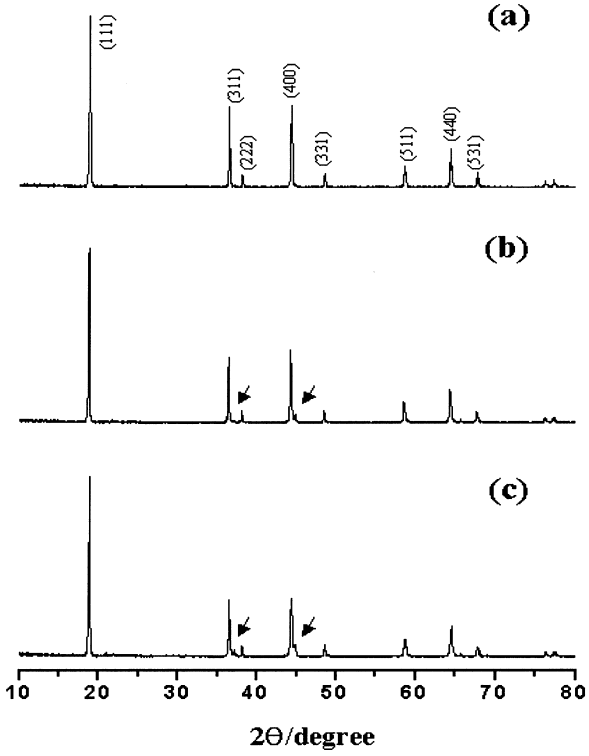

Fig. 5. X-ray diffraction patterns of $Li_{1.02}Mg_{0.1}Mn_{1.9}O_{4-y}S_y$ powder prepared at various sulfur contents. The gel precursors were calcined at 750°C in O_2: (a) $Li_{1.02}Mg_{0.1}Mn_{1.9}O_{3.99}S_{0.01}$; (b) $Li_{1.02}Mg_{0.1}Mn_{1.9}O_{3.98}S_{0.02}$; (c) $Li_{1.02}Mg_{0.1}Mn_{1.9}O_{3.97}S_{0.03}$.

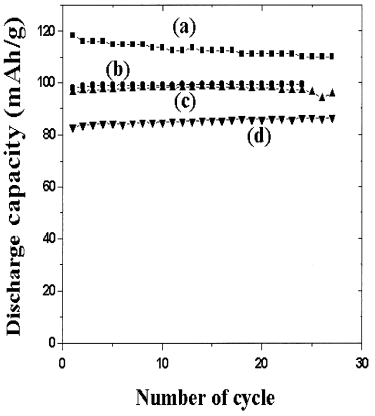

Fig. 6. Specific discharge capacity vs. cycle number for the Li/$LiPF_6$-EC/DMC (vol. 1:1)/$Li_{1.02}Mg_xMn_{2-x}O_{4-y}S_y$ calcined at 750°C in O_2: cycling carried out galvanostatically at constant charge-discharge current density of 1 mA h cm^{-2} between 3.0 and 4.3 V at room temperature: (a) $Li_{1.02}Mn_2O_4$; (b) $Li_{1.02}Mg_{0.1}Mn_{1.9}O_4$; (c) $Li_{1.02}Mn_2O_{3.99}S_{0.01}$; (d) $Li_{1.02}Mg_{0.1}Mn_{1.9}O_{3.99}S_{0.01}$.

formation of impurities. From the above experiments, it is found that highly crystallized $LiMn_2O_4$ is synthesized when x and y are 0.1.

3.2. Electrochemical characterization of synthesized materials

Electrodes were fabricated using the synthesized $Li_{1.02}Mg_xMn_{2-x}O_{4-y}S_y$ powders ($x = 0, 0.1$ and $y = 0, 0.01$) and the charge-discharge properties were evaluated. Charge-discharge curves measured in the operating potential range 4.4–3.0 V are shown in Fig. 6. The initial capacity of the doped powders decreases because of the decrease in the amount of extractable lithium. The removal of lithium from the spinel manganese oxides is accompanied by an oxidation of Mn^{3+} to Mn^{4+} [28] Given that Mg^{2+} ions cannot be oxidized in this potential range, the amount of removable lithium is determined by the Mn^{3+} content. Thus, only $(1.02 - x)$Li can be extracted from $Li_{1.02}Mg_xMn_{2-x}O_4$. The discharge capacity measurements indicate that the content of suitable dopant should not be too large to obtain a high discharge capacity. The $Li_{1.02}Mn_2O_4$ cell delivers an initial discharge capacity of 118 mA h g^{-1}, but this value decreases gradually with cycling, as observed by other workers [29,30]. For $Li_{1.02}Mg_{0.1}Mn_{1.9}O_4$ and $Li_{1.02}Mn_2O_{3.99}S_{0.01}$ cells, however, the initial capacity is 99 mA h g^{-1} and is retained after 28 cycles, as shown in Fig. 6(b) and (c). $Li_{1.02}Mg_{0.1}Mn_{1.9}O_{3.99}S_{0.01}$ only delivers 85 mA h g^{-1} although capacity fading is not detected after 28 cycles. This is because the oxidation state of Mn is increased not only by the substitution of Mg^{2+} for Mn, but also by that of S for O. The material exhibits very good capacity retention due to improvement in the stability of cation sites (16d) and anion sites (32e).

The enhanced cycle performance of electrodes by doping is achieved by stabilizing the octahedral sites in the spinel skeleton structure with doped metal cations.

4. Conclusions

A spinel oxysulfide $Li_{1.02}Mg_{0.1}Mn_{1.9}O_{3.99}S_{0.01}$ have been synthesized using a sol–gel method and the structural and electrochemical properties of the synthesized product are evaluated to chracterize the synthesized material. The $Li_{1.02}Mg_{0.1}Mn_{1.9}O_{3.99}S_{0.01}$ powder is identified as a single-phase spinel with a space group *Fd3m*. The powder is shaped into a well-developed octahedral structure which is bounded by eight (1 1 1) planes. The effect of Mg and S doping in $LiMn_2O_4$ has also been examined as a function of the amount of Mg and S dopant. The crystallinity of $LiMn_2O_4$ deteriorates with increase in Mg doping. A $Li_{1.02}Mn_2O_4$ cell delivers an initial discharge capacity of 118 mA h g^{-1}, but the capacity decreases gradually with cycling. For $Li_{1.02}Mg_{0.1}Mn_{1.9}O_4$ and $Li_{1.02}Mn_2O_{3.99}S_{0.01}$ cells, however, the initial capacity is 99 mA h g^{-1} and the capacity is retained after 28 cycles. A $Li_{1.02}Mg_{0.1}Mn_{1.9}O_{3.99}S_{0.01}$ cell only delivers 85 mA h g^{-1} although capacity fading is not detected after 28 cycles. The improvement in the cycle performance of the electrode by the doping is achieved by stabilizing the octahedral sites in the spinel skeleton structure with the doped metal cations.

Acknowledgements

The authors acknowledge the financial support of the Korea Research Foundation made in the program year of 1998.

References

[1] J.R. Dahn, U.V. Scken, C.A. Michal, Solid State Ionics 44 (1990) 87.
[2] D. Guyomard, J.M. Tarascon, Solid State Ionics 69 (9994) 222.
[3] M.M. Thackeray, P.J. Johnson, L.A. de piccioto, P.G. Bruce, J.B. Goodenough, Mater. Res. Bull. 19 (1984) 179.
[4] T. Ohuzuka, M. Kitagawa, T. Hirai, J. Electrochem. Soc. 137 (1990) 769.
[5] J.M. Tarascon, E. Wang, F.K. Shokoohi, W.R. Mckinnon, S. Colson, J. Electrochem. Soc. 138 (1991) 2859.
[6] T. Ohzuku, M. Kitagawa, T. Hirai, J. Electrochem. Soc. 137 (1990) 769.
[7] M.M. Thackeray, J. Electrochem. Soc. 142 (1995) 2558.
[8] R.J. Gummow, A. Kock, M.M. Thackeray, Solid State Ionics 69 (1994) 59.
[9] D.H. Jang, Y.J. Shin, S.M. Oh, J. Electrochem. Soc. 143 (1996) 2204.
[10] Y. Xia, Y. Zhou, M. Yoshio, J. Electrochem. Soc. 144 (1997) 2593.
[11] M.M. Thackery, Prog. Solid State Chem. 25 (1997) 1.
[12] A.D. Roberston, S.H. Lu, W.F. Averill, W.F. Howard Jr., J. Electrochem. Soc. 144 (1997) 3500.
[13] A.D. Roberston, S.H. Lu, W.F. Howard Jr., J. Electrochem. Soc. 144 (1997) 3505.

[14] L. Guohua, H. Ikuta, T. Uchida, M. Wakihara, J. Electrochem. Soc. 143 (1996) 178.
[15] K. Amine, H. Tukamoto, H. Yasada, Y. Fujita, J. Electrochem. Soc. 143 (1996) 1607.
[16] G.G. Amatucci, US Patent No. 5,759,720 (1998).
[17] S.H. Park, K.S. Park, Y.K. Sun, K.S. Nahm, J. Electrochem. Soc. 147 (2000) 2116.
[18] Y.S. Lee, Y.K. Sun, K.S. Nahm, Solid State Ionics 109 (1998) 285.
[19] G.H. Jeffery, J. Bassett, J. Mendham, R.C. Denney, Vogel's Textbook of Quantitative Chemical Analysis, Longman, New York, 1989.
[20] M.M. Thackeray, L.A. de Picciotto, A. de Kock, P.J. Johnson, V.A. Nicholas, K.T. Adendorff, J. Power Sour. 21 (1986) 1.
[21] D.S. Ahn, M.Y. Song, J. Electrochem. Soc. 147 (2000) 874.
[22] D. Fatcasiu, J.Q. Li, S. Cameron, Appl. Catal. 154 (1997) 173.
[23] J.M. Tarascon, E. Wang, F.K. Shockophi, W.R. Mekinon, S. Colson, J. Electrochem. Soc. 138 (1991) 2859.
[24] R.T. Cygan, H.R. Westrich, D.H. Doughty, Mater. Res. Soc. Symp. Proc. 393 (1995) 113.
[25] H.P. Klug, L.E. Alexander, X-ray Diffraction Procedure for Polycrystalline and Amorphous Materials, 2nd Edition, Wiley, New York, 1974.
[26] P. Barboux, J.M. Tarascon, F.K. Shokoohi, J. Solid State Chem. 94 (1991) 185.
[27] T. Tsumura, A. Shimizu, M. Inagaki, Solid State Ionics 90 (1996) 197.
[28] D. Guyomard, J.M. Tarascon, Solid State Ionics 69 (1996) 222.
[29] D.H. Jang, Y.J. Shin, S.M. Oh, J. Electrochem. Soc. 143 (1996) 2204.
[30] V. Manev, B. Herr, A. Nassalevska, J. Power Sour. 57 (1995) 99.